

# High-Performance Large-Scale Image Recognition Without Normalization

Andrew Brock<sup>1</sup> Soham De<sup>1</sup> Samuel L. Smith<sup>1</sup> Karen Simonyan<sup>1</sup>

## Abstract

Batch normalization is a key component of most image classification models, but it has many undesirable properties stemming from its dependence on the batch size and interactions between examples. Although recent work has succeeded in training deep ResNets without normalization layers, these models do not match the test accuracies of the best batch-normalized networks, and are often unstable for large learning rates or strong data augmentations. In this work, we develop an adaptive gradient clipping technique which overcomes these instabilities, and design a significantly improved class of Normalizer-Free ResNets. Our smaller models match the test accuracy of an EfficientNet-B7 on ImageNet while being up to  $8.7\times$  faster to train, and our largest models attain a new state-of-the-art top-1 accuracy of 86.5%. In addition, Normalizer-Free models attain significantly better performance than their batch-normalized counterparts when fine-tuning on ImageNet after large-scale pre-training on a dataset of 300 million labeled images, with our best models obtaining an accuracy of 89.2%. Code and pretrained models are available at <https://github.com/deepmind/deepmind-research/tree/master/nfnets>

## 1. Introduction

The vast majority of recent models in computer vision are variants of deep residual networks (He et al., 2016b;a), trained with batch normalization (Ioffe & Szegedy, 2015). The combination of these two architectural innovations has enabled practitioners to train significantly deeper networks which can achieve higher accuracies on both the training set and the test set. Batch normalization also smoothens the loss landscape (Santurkar et al., 2018), which enables stable

<sup>1</sup>DeepMind, London, United Kingdom. Correspondence to: Andrew Brock <ajbrock@deepmind.com>.

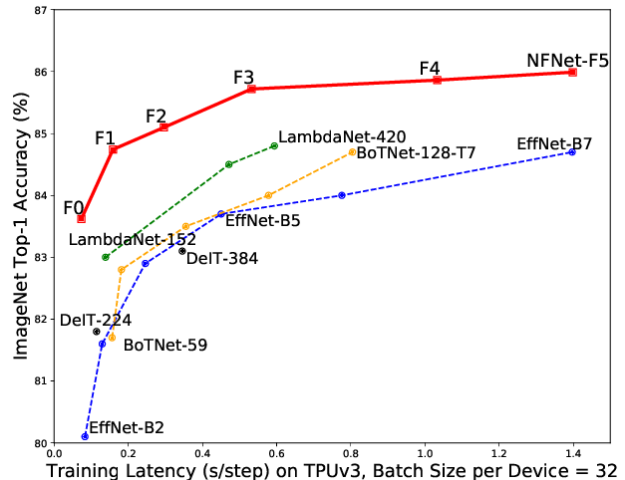


Figure 1. ImageNet Validation Accuracy vs Training Latency. All numbers are single-model, single crop. Our NFNet-F1 model achieves comparable accuracy to an EffNet-B7 while being  $8.7\times$  faster to train. Our NFNet-F5 model has similar training latency to EffNet-B7, but achieves a state-of-the-art 86.0% top-1 accuracy on ImageNet. We further improve on this using Sharpness Aware Minimization (Foret et al., 2021) to achieve 86.5% top-1 accuracy.

training with larger learning rates and at larger batch sizes (Bjorck et al., 2018; De & Smith, 2020), and it can have a regularizing effect (Hoffer et al., 2017; Luo et al., 2018).

However, batch normalization has three significant practical disadvantages. First, it is a surprisingly expensive computational primitive, which incurs memory overhead (Rota Bulò et al., 2018), and significantly increases the time required to evaluate the gradient in some networks (Gitman & Ginsburg, 2017). Second, it introduces a discrepancy between the behaviour of the model during training and at inference time (Summers & Dinneen, 2019; Singh & Shrivastava, 2019), introducing hidden hyper-parameters that have to be tuned. Third, and most importantly, batch normalization breaks the independence between training examples in the minibatch.

This third property has a range of negative consequences. For instance, practitioners have found that batch normalized networks are often difficult to replicate precisely on different hardware, and batch normalization is often the cause of subtle implementation errors, especially during distributed training (Pham et al., 2019). Furthermore, batch normal-

ization cannot be used for some tasks, since the interaction between training examples in a batch enables the network to ‘cheat’ certain loss functions. For example, batch normalization requires specific care to prevent information leakage in some contrastive learning algorithms (Chen et al., 2020; He et al., 2020). This is a major concern for sequence modeling tasks as well, which has driven language models to adopt alternative normalizers (Ba et al., 2016; Vaswani et al., 2017). The performance of batch-normalized networks can also degrade if the batch statistics have a large variance during training (Shen et al., 2020). Finally, the performance of batch normalization is sensitive to the batch size, and batch normalized networks perform poorly when the batch size is too small (Hoffer et al., 2017; Ioffe, 2017; Wu & He, 2018), which limits the maximum model size we can train on finite hardware. We expand on the challenges associated with batch normalization in Appendix B.

Therefore, although batch normalization has enabled the deep learning community to make substantial gains in recent years, we anticipate that in the long term it is likely to impede progress. We believe the community should seek to identify a simple alternative which achieves competitive test accuracies and can be used for a wide range of tasks. Although a number of alternative normalizers have been proposed (Ba et al., 2016; Wu & He, 2018; Huang et al., 2020), these alternatives often achieve inferior test accuracies and introduce their own disadvantages, such as additional compute costs at inference. Fortunately, in recent years two promising research themes have emerged. The first studies the origin of the benefits of batch normalization during training (Balduzzi et al., 2017; Santurkar et al., 2018; Bjorck et al., 2018; Luo et al., 2018; Yang et al., 2019; Jacot et al., 2019; De & Smith, 2020), while the second seeks to train deep ResNets to competitive accuracies without normalization layers (Hanin & Rolnick, 2018; Zhang et al., 2019a; De & Smith, 2020; Shao et al., 2020; Brock et al., 2021).

A key theme in many of these works is that it is possible to train very deep ResNets without normalization by suppressing the scale of the hidden activations on the residual branch. The simplest way to achieve this is to introduce a learnable scalar at the end of each residual branch, initialized to zero (Goyal et al., 2017; Zhang et al., 2019a; De & Smith, 2020; Bachlechner et al., 2020). However this trick alone is not sufficient to obtain competitive test accuracies on challenging benchmarks. Another line of work has shown that ReLU activations introduce a ‘mean shift’, which causes the hidden activations of different training examples to become increasingly correlated as the network depth increases (Huang et al., 2017; Jacot et al., 2019). In a recent work, Brock et al. (2021) introduced “Normalizer-Free” ResNets, which suppress the residual branch at initialization and apply Scaled Weight Standardization (Qiao et al., 2019) to remove the mean shift. With additional regularization, these unnormal-

ized networks match the performance of batch-normalized ResNets (He et al., 2016a) on ImageNet (Russakovsky et al., 2015), but they are not stable at large batch sizes and do not match the performance of EfficientNets (Tan & Le, 2019), the current state of the art (Gong et al., 2020). This paper builds on this line of work and seeks to address these central limitations. Our main contributions are as follows:

- We propose Adaptive Gradient Clipping (AGC), which clips gradients based on the *unit-wise ratio of gradient norms to parameter norms*, and we demonstrate that AGC allows us to train Normalizer-Free Networks with larger batch sizes and stronger data augmentations.
- We design a family of Normalizer-Free ResNets, called NFNet, which set new state-of-the-art validation accuracies on ImageNet for a range of training latencies (See Figure 1). Our NFNet-F1 model achieves similar accuracy to EfficientNet-B7 while being  $8.7\times$  faster to train, and our largest model sets a new overall state of the art without extra data of 86.5% top-1 accuracy.
- We show that NFNet achieve substantially higher validation accuracies than batch-normalized networks when fine-tuning on ImageNet after pre-training on a large private dataset of 300 million labelled images. Our best model achieves 89.2% top-1 after fine-tuning.

The paper is structured as follows. We discuss the benefits of batch normalization in Section 2, and recent work seeking to train ResNets without normalization in Section 3. We introduce AGC in Section 4, and we describe how we developed our new state-of-the-art architectures in Section 5. Finally, we present our experimental results in Section 6.

## 2. Understanding Batch Normalization

In order to train networks without normalization to competitive accuracy, we must understand the benefits batch normalization brings during training, and identify alternative strategies to recover these benefits. Here we list the four main benefits which have been identified by prior work.

### Batch normalization downscales the residual branch:

The combination of skip connections (Srivastava et al., 2015; He et al., 2016b;a) and batch normalization (Ioffe & Szegedy, 2015) enables us to train significantly deeper networks with thousands of layers (Zhang et al., 2019a). This benefit arises because batch normalization, when placed on the residual branch (as is typical), reduces the scale of hidden activations on the residual branches at initialization (De & Smith, 2020). This biases the signal towards the skip path, which ensures that the network has well-behaved gradients early in training, enabling efficient optimization (Balduzzi et al., 2017; Hanin & Rolnick, 2018; Yang et al., 2019).

**Batch normalization eliminates mean-shift:** Activation functions like ReLUs or GELUs (Hendrycks & Gimpel, 2016), which are not anti-symmetric, have non-zero mean activations. Consequently, the inner product between the activations of independent training examples immediately after the non-linearity is typically large and positive, even if the inner product between the input features is close to zero. This issue compounds as the network depth increases, and introduces a ‘mean-shift’ in the activations of different training examples on any single channel proportional to the network depth (De & Smith, 2020), which can cause deep networks to predict the same label for all training examples at initialization (Jacot et al., 2019). Batch normalization ensures the mean activation on each channel is zero across the current batch, eliminating mean shift (Brock et al., 2021).

**Batch normalization has a regularizing effect:** It is widely believed that batch normalization also acts as a regularizer enhancing test set accuracy, due to the noise in the batch statistics which are computed on a subset of the training data (Luo et al., 2018). Consistent with this perspective, the test accuracy of batch-normalized networks can often be improved by tuning the batch size, or by using ghost batch normalization in distributed training (Hoffer et al., 2017).

**Batch normalization allows efficient large-batch training:** Batch normalization smoothens the loss landscape (Santurkar et al., 2018), and this increases the largest stable learning rate (Bjorck et al., 2018). While this property does not have practical benefits when the batch size is small (De & Smith, 2020), the ability to train at larger learning rates is essential if one wishes to train efficiently with large batch sizes. Although large-batch training does not achieve higher test accuracies within a fixed epoch budget (Smith et al., 2020), it does achieve a given test accuracy in fewer parameter updates, significantly improving training speed when parallelized across multiple devices (Goyal et al., 2017).

### 3. Towards Removing Batch Normalization

Many authors have attempted to train deep ResNets to competitive accuracies without normalization, by recovering one or more of the benefits of batch normalization described above. Most of these works suppress the scale of the activations on the residual branch at initialization, by introducing either small constants or learnable scalars (Hanin & Rolnick, 2018; Zhang et al., 2019a; De & Smith, 2020; Shao et al., 2020). Additionally, Zhang et al. (2019a) and De & Smith (2020) observed that the performance of unnormalized ResNets can be improved with additional regularization. However only recovering these two benefits of batch normalization is not sufficient to achieve competitive test accuracies on challenging benchmarks (De & Smith, 2020).

In this work, we adopt and build on “Normalizer-Free

ResNets” (NF-ResNets) (Brock et al., 2021), a class of pre-activation ResNets (He et al., 2016a) which can be trained to competitive training and test accuracies without normalization layers. NF-ResNets employ a residual block of the form  $h_{i+1} = h_i + \alpha f_i(h_i/\beta_i)$ , where  $h_i$  denotes the inputs to the  $i^{\text{th}}$  residual block, and  $f_i$  denotes the function computed by the  $i^{\text{th}}$  residual branch. The function  $f_i$  is parameterized to be variance preserving at initialization, such that  $\text{Var}(f_i(z)) = \text{Var}(z)$  for all  $i$ . The scalar  $\alpha$  specifies the rate at which the variance of the activations increases after each residual block (at initialization), and is typically set to a small value like  $\alpha = 0.2$ . The scalar  $\beta_i$  is determined by predicting the standard deviation of the inputs to the  $i^{\text{th}}$  residual block,  $\beta_i = \sqrt{\text{Var}(h_i)}$ , where  $\text{Var}(h_{i+1}) = \text{Var}(h_i) + \alpha^2$ , except for transition blocks (where spatial downsampling occurs), for which the skip path operates on the downsampled input ( $h_i/\beta_i$ ), and the expected variance is reset after the transition block to  $h_{i+1} = 1 + \alpha^2$ . The outputs of squeeze-excite layers (Hu et al., 2018) are multiplied by a factor of 2. Empirically, Brock et al. (2021) found it was also beneficial to include a learnable scalar initialized to zero at the end of each residual branch (‘SkipInit’ (De & Smith, 2020)).

In addition, Brock et al. (2021) prevent the emergence of a mean-shift in the hidden activations by introducing Scaled Weight Standardization (a minor modification of Weight Standardization (Huang et al., 2017; Qiao et al., 2019)). This technique reparameterizes the convolutional layers as:

$$\hat{W}_{ij} = \frac{W_{ij} - \mu_i}{\sqrt{N}\sigma_i}, \quad (1)$$

where  $\mu_i = (1/N) \sum_j W_{ij}$ ,  $\sigma_i^2 = (1/N) \sum_j (W_{ij} - \mu_i)^2$ , and  $N$  denotes the fan-in. The activation functions are also scaled by a non-linearity specific scalar gain  $\gamma$ , which ensures that the combination of the  $\gamma$ -scaled activation function and a Scaled Weight Standardized layer is variance preserving. For ReLUs,  $\gamma = \sqrt{2/(1 - (1/\pi))}$  (Arpit et al., 2016). We refer the reader to Brock et al. (2021) for a description of how to compute  $\gamma$  for other non-linearities.

With additional regularization (Dropout (Srivastava et al., 2014) and Stochastic Depth (Huang et al., 2016)), Normalizer-Free ResNets match the test accuracies achieved by batch normalized pre-activation ResNets on ImageNet at batch size 1024. They also significantly outperform their batch normalized counterparts when the batch size is very small, but they perform worse than batch normalized networks for large batch sizes (4096 or higher). Crucially, they do not match the performance of state-of-the-art networks like EfficientNets (Tan & Le, 2019; Gong et al., 2020).

## 4. Adaptive Gradient Clipping for Efficient Large-Batch Training

To scale NF-ResNets to larger batch sizes, we explore a range of gradient clipping strategies (Pascanu et al., 2013). Gradient clipping is often used in language modeling to stabilize training (Merity et al., 2018), and recent work shows that it allows training with larger learning rates compared to gradient descent, accelerating convergence (Zhang et al., 2020). This is particularly important for poorly conditioned loss landscapes or when training with large batch sizes, since in these settings the optimal learning rate is constrained by the maximum stable learning rate (Smith et al., 2020). We therefore hypothesize that gradient clipping should help scale NF-ResNets efficiently to the large-batch setting.

Gradient clipping is typically performed by constraining the norm of the gradient (Pascanu et al., 2013). Specifically, for gradient vector  $G = \partial L / \partial \theta$ , where  $L$  denotes the loss and  $\theta$  denotes a vector with all model parameters, the standard clipping algorithm clips the gradient before updating  $\theta$  as:

$$G \rightarrow \begin{cases} \lambda \frac{G}{\|G\|} & \text{if } \|G\| > \lambda, \\ G & \text{otherwise.} \end{cases} \quad (2)$$

The clipping threshold  $\lambda$  is a hyper-parameter which must be tuned. Empirically, we found that while this clipping algorithm enabled us to train at higher batch sizes than before, training stability was extremely sensitive to the choice of the clipping threshold, requiring fine-grained tuning when varying the model depth, the batch size, or the learning rate.

To overcome this issue, we introduce ‘‘Adaptive Gradient Clipping’’ (AGC), which we now describe. Let  $W^\ell \in \mathbb{R}^{N \times M}$  denote the weight matrix of the  $\ell^{\text{th}}$  layer,  $G^\ell \in \mathbb{R}^{N \times M}$  denote the gradient with respect to  $W^\ell$ , and  $\|\cdot\|_F$  denote the Frobenius norm, i.e.,  $\|W^\ell\|_F = \sqrt{\sum_i \sum_j (W_{i,j}^\ell)^2}$ . The AGC algorithm is motivated by the observation that the ratio of the norm of the gradients  $G^\ell$  to the norm of the weights  $W^\ell$  of layer  $\ell$ ,  $\frac{\|G^\ell\|_F}{\|W^\ell\|_F}$ , provides a simple measure of how much a single gradient descent step will change the original weights  $W^\ell$ . For instance, if we train using gradient descent without momentum, then  $\frac{\|\Delta W^\ell\|}{\|W^\ell\|} = h \frac{\|G^\ell\|_F}{\|W^\ell\|_F}$ , where the parameter update for the  $\ell^{\text{th}}$  layer is given by  $\Delta W^\ell = -hG^\ell$ , and  $h$  is the learning rate.

Intuitively, we expect training to become unstable if  $(\|\Delta W^\ell\| / \|W^\ell\|)$  is large, which motivates a clipping strategy based on the ratio  $\frac{\|G^\ell\|_F}{\|W^\ell\|_F}$ . However in practice, we clip gradients based on the *unit-wise ratios* of gradient norms to parameter norms, which we found to perform better empirically than taking layer-wise norm ratios. Specifically, in our AGC algorithm, each unit  $i$  of the gradient of the  $\ell$ -th layer

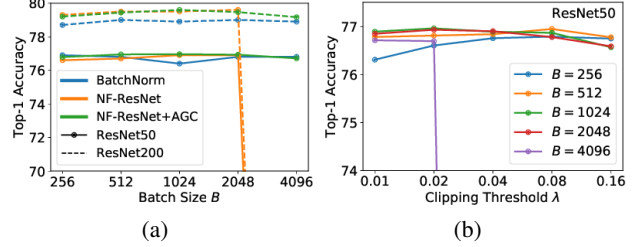


Figure 2. (a) AGC efficiently scales NF-ResNets to larger batch sizes. (b) The performance across different clipping thresholds  $\lambda$ .

$G_i^\ell$  (defined as the  $i^{\text{th}}$  row of matrix  $G^\ell$ ) is clipped as:

$$G_i^\ell \rightarrow \begin{cases} \lambda \frac{\|W_i^\ell\|_F}{\|G_i^\ell\|_F} G_i^\ell & \text{if } \frac{\|G_i^\ell\|_F}{\|W_i^\ell\|_F} > \lambda, \\ G_i^\ell & \text{otherwise.} \end{cases} \quad (3)$$

The clipping threshold  $\lambda$  is a scalar hyperparameter, and we define  $\|W_i^\ell\|_F^* = \max(\|W_i^\ell\|_F, \epsilon)$ , with default  $\epsilon = 10^{-3}$ , which prevents zero-initialized parameters from always having their gradients clipped to zero. For parameters in convolutional filters, we evaluate the unit-wise norms over the fan-in extent (including the channel and spatial dimensions). Using AGC, we can train NF-ResNets stably with larger batch sizes (up to 4096), as well as with very strong data augmentations like RandAugment (Cubuk et al., 2020) for which NF-ResNets without AGC fail to train (Brock et al., 2021). Note that the optimal clipping parameter  $\lambda$  may depend on the choice of optimizer, learning rate and batch size. Empirically, we find  $\lambda$  should be smaller for larger batches.

AGC is closely related to a recent line of work studying ‘‘normalized optimizers’’ (You et al., 2017; Bernstein et al., 2020; You et al., 2019), which ignore the scale of the gradient by choosing an adaptive learning rate inversely proportional to the gradient norm. In particular, You et al. (2017) propose LARS, a momentum variant which sets the norm of the parameter update to be a fixed ratio of the parameter norm, completely ignoring the gradient magnitude. AGC can be interpreted as a relaxation of normalized optimizers, which imposes a maximum update size based on the parameter norm but does not simultaneously impose a lower-bound on the update size or ignore the gradient magnitude. Although we are also able to stably train at high batch sizes with LARS, we found that doing so degrades performance.

### 4.1. Ablations for Adaptive Gradient Clipping (AGC)

We now present a range of ablations designed to test the efficacy of AGC. We performed experiments on pre-activation NF-ResNet-50 and NF-ResNet-200 on ImageNet, trained using SGD with Nesterov’s Momentum for 90 epochs at a range of batch sizes between 256 and 4096. As in Goyal et al. (2017) we use a base learning rate of 0.1 for batch size 256, which is scaled linearly with the batch size. We

consider a range of  $\lambda$  values [0.01, 0.02, 0.04, 0.08, 0.16].

In Figure 2(a), we compare batch-normalized ResNets to NF-ResNets with and without AGC. We show test accuracy at the best clipping threshold  $\lambda$  for each batch size. We find that AGC helps scale NF-ResNets to large batch sizes while maintaining performance comparable or better than batch-normalized networks on both ResNet50 and ResNet200. As anticipated, the benefits of using AGC are smaller when the batch size is small. In Figure 2(b), we show performance for different clipping thresholds  $\lambda$  across a range of batch sizes on ResNet50. We see that smaller (stronger) clipping thresholds are necessary for stability at higher batch sizes. We provide additional ablation details in Appendix D.

Next, we study whether or not AGC is beneficial for all layers. Using batch size 4096 and a clipping threshold  $\lambda = 0.01$ , we remove AGC from different combinations of the first convolution, the final linear layer, and every block in any given set of the residual stages. For example, one experiment may remove clipping in the linear layer and all the blocks in the second and fourth stages. Two key trends emerge: first, it is always better to not clip the final linear layer. Second, it is often possible to train stably without clipping the initial convolution, but the weights of all four stages must be clipped to achieve stability when training at batch size 4096 with the default learning rate of 1.6. For the rest of this paper (and for our ablations in Figure 2), we apply AGC to every layer except for the final linear layer.

## 5. Normalizer-Free Architectures with Improved Accuracy and Training Speed

In the previous section we introduced AGC, a gradient clipping method which allows us to train efficiently with large batch sizes and strong data augmentations. Equipped with this technique, we now seek to design Normalizer-Free architectures with state-of-the-art accuracy and training speed.

The current state of the art on image classification is generally held by the EfficientNet family of models (Tan & Le, 2019), which are based on a variant of inverted bottleneck blocks (Sandler et al., 2018) with a backbone and model scaling strategy derived from neural architecture search. These models are optimized to maximize test accuracy while minimizing parameter and FLOP counts, but their low theoretical compute complexity does not translate into improved training speed on modern accelerators. Despite having 10x fewer FLOPS than a ResNet-50, an EffNet-B0 has similar training latency and final performance when trained on GPU or TPU.

The choice of which metric to optimize— theoretical FLOPS, inference latency on a target device, or training latency on an accelerator—is a matter of preference, and the nature of each metric will yield different design requirements. In this work we choose to focus on manually designing models which

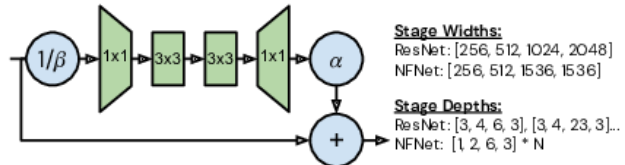


Figure 3. Summary of NFNet bottleneck block design and architectural differences. See Figure 5 in Appendix C for more details.

Table 1. NFNet family depths, drop rates, and input resolutions.

Variant	Depth	Dropout	Train	Test
F0	[1, 2, 6, 3]	0.2	192px	256px
F1	[2, 4, 12, 6]	0.3	224px	320px
F2	[3, 6, 18, 9]	0.4	256px	352px
F3	[4, 8, 24, 12]	0.4	320px	416px
F4	[5, 10, 30, 15]	0.5	384px	512px
F5	[6, 12, 36, 18]	0.5	416px	544px
F6	[7, 14, 42, 21]	0.5	448px	576px

are optimized for training latency on existing accelerators, as in Radosavovic et al. (2020). It is possible that future accelerators may be able to take full advantage of the potential training speed that largely goes unrealized with models like EfficientNets, so we believe this direction should not be ignored (Hooker, 2020), however we anticipate that developing models with improved training speed on current hardware will be beneficial for accelerating research. We note that accelerators like GPU and TPU tend to favor dense computation, and while there are differences between these two platforms, they have enough in common that models designed for one device are likely to train fast on the other.

We therefore explore the space of model design by manually searching for design trends which yield improvements to the pareto front of holdout top-1 on ImageNet against actual training latency on device. This section describes the changes which we found to work well to this end (with more details in Appendix C), while the ideas which we found to work poorly are described in Appendix E. A summary of these modifications is presented in Figure 3, and the effect they have on holdout accuracy is presented in Table 2.

We begin with an SE-ResNeXt-D model (Xie et al., 2017; Hu et al., 2018; He et al., 2019) with GELU activations (Hendrycks & Gimpel, 2016), which we found to be a surprisingly strong baseline for Normalizer-Free Networks. We make the following changes. First, we set the group width (the number of channels each output unit is connected to) in the  $3 \times 3$  convs to 128, regardless of block width. Smaller group widths reduce theoretical FLOPS, but the reduction in compute density means that on many modern accelerators no actual speedup is realized. On TPUv3 for example, an SE-ResNeXt-50 with a group width of 8 trains at the same

Table 2. The effect of architectural modifications and data augmentation on ImageNet Top-1 accuracy (averaged over 3 seeds).

	F0	F1	F2	F3
Baseline	80.4	81.7	82.0	82.3
+ Modified Width	80.9	81.8	82.0	82.3
+ Second Conv	81.3	82.2	82.4	82.7
+ MixUp	82.2	82.9	83.1	83.5
+ RandAugment	83.2	84.6	84.8	85.0
+ CutMix	<b>83.6</b>	<b>84.7</b>	<b>85.1</b>	<b>85.7</b>
Default Width + Augs	83.1	84.5	85.0	85.5

speed as an SE-ResNeXt-50 with a group width of 128 unless the per-device batch size is 128 or larger (Google, 2021), which is often not realizable due to memory constraints.

Next, we make two changes to the model backbone. First, we note that the default depth scaling pattern for ResNets (e.g., the method by which one increases depth to construct a ResNet101 or ResNet200 from a ResNet50) involves non-uniformly increasing the number of layers in the second and third stages, while maintaining 3 blocks in the first and fourth stages, where ‘stage’ refers to a sequence of residual blocks whose activations are the same width and have the same resolution. We find that this strategy is suboptimal. Layers in early stages operate at higher resolution, require more memory and compute, and tend to learn localized, task-general features (Krizhevsky et al., 2012), while layers in later stages operate at lower resolutions, contain most of the model’s parameters, and learn more task-specific features (Raghu et al., 2017a). However, being overly parsimonious with early stages (such as through aggressive downsampling) can hurt performance, since the model needs enough capacity to extract good local features (Raghu et al., 2017b). It is also desirable to have a simple scaling rule for constructing deeper variants (Tan & Le, 2019). With these principles in mind, we explored several choices of backbone for our smallest model variant, named F0, before settling on the simple pattern [1, 2, 6, 3] (indicating how many bottleneck blocks to allocate to each stage). We construct deeper variants by multiplying the depth of each stage by a scalar  $N$ , so that, for example, variant F1 has a depth pattern [2, 4, 12, 6], and variant F4 has a depth pattern [5, 10, 30, 15].

In addition, we reconsider the default width pattern in ResNets, where the first stage has 256 channels which are doubled at each subsequent stage, resulting in a pattern [256, 512, 1024, 2048]. Employing our depth patterns described above, we considered a range of alternative patterns (taking inspiration from Radosavovic et al. (2020)) but found that only one choice was better than this default: [256, 512, 1536, 1536]. This width pattern is designed to increase capacity in the third stage while slightly reducing capacity in the fourth stage, roughly preserving training

speed. Consistent with our chosen depth pattern and the default design of ResNets, we find that the third stage tends to be the best place to add capacity, which we hypothesize is due to this stage being deep enough to have a large receptive field and access to deeper levels of the feature hierarchy, while having a slightly higher resolution than the final stage.

We also consider the structure of the bottleneck residual block itself. We considered a variety of pre-existing and novel modifications (see Appendix E) but found that the best improvement came from adding an additional  $3 \times 3$  grouped conv after the first (with accompanying nonlinearity). This additional convolution minimally impacts FLOPS and has almost no impact on training time on our target accelerators.

Finally, we establish a scaling strategy to produce model variants at different compute budgets. The EfficientNet scaling strategy (Tan & Le, 2019) is to jointly scale model width, depth, and input resolution, which works extremely well for base models with very slim MobileNet-like backbones. However we find that width scaling is ineffective for ResNet backbones, consistent with Bello (2021), who attain strong performance when only scaling depth and input resolution. We therefore also adopt the latter strategy, using the fixed width pattern mentioned above, scaling depth as described above, and scaling training resolution such that each variant is approximately half as fast to train as its predecessor. Following Touvron et al. (2019), we evaluate images at inference at a slightly higher resolution than we train at, chosen for each variant as approximately 33% larger than the train resolution. We do not fine-tune at this higher resolution.

We also find that it is helpful to increase the regularization strength as the model capacity rises. However modifying the weight decay or stochastic depth rate was not effective, and instead we scale the drop rate of Dropout (Srivastava et al., 2014), following Tan & Le (2019). This step is particularly important as our models lack the implicit regularization of batch normalization, and without explicit regularization tend to dramatically overfit. Our resulting models are highly performant and, despite being optimized for training latency, remain competitive with larger EfficientNet variants in terms of FLOPs vs accuracy (although not in terms of parameters vs accuracy), as shown in Figure 4 in Appendix A.

## 5.1. Summary

Our training recipe can be summarized as follows: First, apply the Normalizer-Free setup of Brock et al. (2021) to an SE-ResNeXt-D, with modified width and depth patterns, and a second spatial convolution. Second, apply AGC to every parameter except for the linear weight of the classifier layer. For batch size 1024 to 4096, set  $\lambda = 0.01$ , and make use of strong regularization and data augmentation. See Table 1 for additional information on each model variant.

## 6. Experiments

### 6.1. Evaluating NFNets on ImageNet

We now turn our attention to evaluating our NFNet models on ImageNet, beginning with an ablation of our architectural modifications when training for 360 epochs at batch size 4096. We use Nesterov’s Momentum with a momentum coefficient of 0.9, AGC as described in Section 4 with a clipping threshold of 0.01, and a learning rate which linearly increases from 0 to 1.6 over 5 epochs, before decaying to zero with cosine annealing (Loshchilov & Hutter, 2017). From the first three rows of Table 2, we can see that the two changes we make to the model each result in slight improvements to performance with only minor changes in training latency (See Table 7 in the Appendix for latencies).

Next, we evaluate the effects of progressively adding stronger augmentations, combining MixUp (Zhang et al., 2017), RandAugment (RA, (Cubuk et al., 2020)) and CutMix (Yun et al., 2019). We apply RA with 4 layers and scale the magnitude with the resolution of the images, following Cubuk et al. (2020). We find that this scaling is particularly important, as if the magnitude is set too high relative to the image size (for example, using a magnitude of 20 on images of resolution 224) then most of the augmented images will be completely blank. See Appendix A for a complete description of these magnitudes and how they are selected. We show in Table 2 that these data augmentations substantially improve performance. Finally, in the last row of Table 2, we additionally present the performance of our full model ablated to use the default ResNet stage widths, demonstrating that our slightly modified pattern in the third and fourth stages does yield improvements under direct comparison.

For completeness, in Table 7 of the Appendix we also report the performance of our model architectures when trained with batch normalization instead of the NF strategy. These models achieve slightly lower test accuracies than their NF counterparts and they are between 20% and 40% slower to train, even when using highly optimized batch normalization implementations without cross-replica syncing. Furthermore, we found that the larger model variants F4 and F5 were not stable when training with batch normalization, with or without AGC. We attribute this to the necessity of using bfloat16 training to fit these larger models in memory, which may introduce numerical imprecision that interacts poorly with the computation of batch normalization statistics.

We provide a detailed summary of the size, training latency (on TPUv3 and V100 with tensorcores), and ImageNet validation accuracy of six model variants, NFNet-F0 through F5, along with comparisons to other models with similar training latencies, in Table 3. Our NFNet-F5 model attains a top-1 validation accuracy of 86.0%, improving over the previous state of the art, EfficientNet-B8 with MaxUp (Gong

et al., 2020) by a small margin, and our NFNet-F1 model matches the 84.7% of EfficientNet-B7 with RA (Cubuk et al., 2020), while being 8.7 times faster to train. See Appendix A for details of how we measure training latency.

Our models also benefit from the recently proposed Sharpness-Aware Minimization (SAM, (Foret et al., 2021)). SAM is not part of our standard training pipeline, as by default it doubles the training time and typically can only be used for distributed training. However we make a small modification to the SAM procedure to reduce this cost to 20-40% increased training time (explained in Appendix A) and employ it to train our two largest model variants, resulting in an NFNet-F5 that attains 86.3% top-1, and an NFNet-F6 that attains 86.5% top-1, substantially improving over the existing state of the art on ImageNet without extra data.

Finally, we also evaluated the performance of our data augmentation strategy on EfficientNets. We find that while RA strongly improves EfficientNets’ performance over baseline augmentation, increasing the number of layers beyond 2 or adding MixUp and CutMix does not further improve their performance, suggesting that our performance improvements are difficult to obtain by simply using stronger data augmentations. We also find that using SGD with cosine annealing instead of RMSProp (Tieleman & Hinton, 2012) with step decay severely degrades EfficientNet performance, indicating that our performance improvements are also not simply due to the selection of a different optimizer.

### 6.2. Evaluating NFNets under Transfer

Unnormalized networks do not share the implicit regularization effect of batch normalization, and on datasets like ImageNet (Russakovsky et al., 2015) they tend to overfit unless explicitly regularized (Zhang et al., 2019a; De & Smith, 2020; Brock et al., 2021). However when pre-training on extremely large scale datasets, such regularization may not only be unnecessary, but also harmful to performance, reducing the model’s ability to devote its full capacity to the training set. We hypothesize that this may make Normalizer-Free networks naturally better suited to transfer learning after large-scale pre-training, and investigate this via pre-training on a large dataset of 300 million labeled images.

We pre-train a range of batch normalized and NF-ResNets for 10 epochs on this large dataset, then fine-tune all layers on ImageNet simultaneously, using a batch size of 2048 and a small learning rate of 0.1 with cosine annealing for 15,000 steps, for input image resolutions in the range [224, 320, 384]. As shown in Table 4, Normalizer-Free networks outperform their Batch-Normalized counterparts in every single case, typically by a margin of around 1% absolute top-1. This suggests that in the transfer learning regime, removing batch normalization can directly benefit final performance.

Table 3. ImageNet Accuracy comparison for NFNets and a representative set of models, including SENet (Hu et al., 2018), LambdaNet, (Bello, 2021), BoTNet (Srinivas et al., 2021), and DeIT (Touvron et al., 2020). Except for results using SAM, our results are averaged over three random seeds. Latencies are given as the time in milliseconds required to perform a single full training step on TPU or GPU (V100).

Model	#FLOPs	#Params	Top-1	Top-5	TPUv3 Train	GPU Train
ResNet-50	4.10B	26.0M	78.6	94.3	41.6ms	35.3ms
EffNet-B0	0.39B	5.3M	77.1	93.3	51.1ms	44.8ms
SENet-50	4.09B	28.0M	79.4	94.6	64.3ms	59.4ms
<b>NFNet-F0</b>	<b>12.38B</b>	<b>71.5M</b>	<b>83.6</b>	<b>96.8</b>	<b>73.3ms</b>	<b>56.7ms</b>
EffNet-B3	1.80B	12.0M	81.6	95.7	129.5ms	116.6ms
LambdaNet-152	–	51.5M	83.0	96.3	138.3ms	135.2ms
SENet-152	19.04B	66.6M	83.1	96.4	149.9ms	151.2ms
BoTNet-110	10.90B	54.7M	82.8	96.3	181.3ms	–
<b>NFNet-F1</b>	<b>35.54B</b>	<b>132.6M</b>	<b>84.7</b>	<b>97.1</b>	<b>158.5ms</b>	<b>133.9ms</b>
EffNet-B4	4.20B	19.0M	82.9	96.4	245.9ms	221.6ms
BoTNet-128-T5	19.30B	75.1M	83.5	96.5	355.2ms	–
<b>NFNet-F2</b>	<b>62.59B</b>	<b>193.8M</b>	<b>85.1</b>	<b>97.3</b>	<b>295.8ms</b>	<b>226.3ms</b>
SENet-350	52.90B	115.2M	83.8	96.6	593.6ms	–
EffNet-B5	9.90B	30.0M	83.7	96.7	450.5ms	458.9ms
LambdaNet-350	–	105.8M	84.5	97.0	471.4ms	–
BoTNet-77-T6	23.30B	53.9M	84.0	96.7	578.1ms	–
<b>NFNet-F3</b>	<b>114.76B</b>	<b>254.9M</b>	<b>85.7</b>	<b>97.5</b>	<b>532.2ms</b>	<b>524.5ms</b>
LambdaNet-420	–	124.8M	84.8	97.0	593.9ms	–
EffNet-B6	19.00B	43.0M	84.0	96.8	775.7ms	868.2ms
BoTNet-128-T7	45.80B	75.1M	84.7	97.0	804.5ms	–
<b>NFNet-F4</b>	<b>215.24B</b>	<b>316.1M</b>	<b>85.9</b>	<b>97.6</b>	<b>1033.3ms</b>	<b>1190.6ms</b>
EffNet-B7	37.00B	66.0M	84.7	97.0	1397.0ms	1753.3ms
DeIT 1000 epochs	–	87.0M	85.2	–	–	–
EffNet-B8+MaxUp	62.50B	87.4M	85.8	–	–	–
<b>NFNet-F5</b>	<b>289.76B</b>	<b>377.2M</b>	<b>86.0</b>	<b>97.6</b>	<b>1398.5ms</b>	<b>2177.1ms</b>
NFNet-F5+SAM	289.76B	377.2M	86.3	97.9	1958.0ms	–
<b>NFNet-F6+SAM</b>	<b>377.28B</b>	<b>438.4M</b>	<b>86.5</b>	<b>97.9</b>	<b>2774.1ms</b>	–

We perform this same experiment using our NFNet models, pre-training an NFNet-F4 and a slightly wider variant which we denote NFNet-F4+ (see Appendix C). As shown in Table 6 of the appendix, with 20 epochs of pre-training our NFNet-F4+ attains an ImageNet top-1 accuracy of 89.2%. This is the second highest validation accuracy achieved to date with extra training data, second only to a strong recent semi-supervised learning baseline (Pham et al., 2020), and the highest accuracy achieved using transfer learning.

### 6.3. Evaluating NFNets as Object Detection Backbones

Finally, we perform experiments to assess the viability of NFNets as backbones for object detection on COCO (Lin et al., 2014). We train models using Mask-RCNN (He et al., 2017) and Feature Pyramid Networks, (Lin et al., 2017),

with training settings similar to Ghiasi et al. (2020), training for 22500 steps using batch size 256, and report Box AP, Mask AP, and training latency in Table 5. NFNets, without any modification, can be successfully substituted into this downstream task in place of batch-normalized ResNet backbones.

## Conclusion

We show for the first time that image recognition models, trained without normalization layers, can not only match the classification accuracies of the best batch normalized models on large-scale datasets but also substantially exceed them, while still being faster to train. To achieve this, we introduce Adaptive Gradient Clipping, a simple clipping algorithm which stabilizes large-batch training and enables us to



Table 4. ImageNet Transfer Top-1 accuracy after pre-training.

	224px	320px	384px
BN-ResNet-50	78.1	79.6	79.9
NF-ResNet-50	<b>79.5</b>	<b>80.9</b>	<b>81.1</b>
BN-ResNet-101	80.8	82.2	82.5
NF-ResNet-101	<b>81.4</b>	<b>82.7</b>	<b>83.2</b>
BN-ResNet-152	81.8	83.1	83.4
NF-ResNet-152	<b>82.7</b>	<b>83.6</b>	<b>84.0</b>
BN-ResNet-200	81.8	83.1	83.5
NF-ResNet-200	<b>82.9</b>	<b>84.1</b>	<b>84.3</b>

Table 5. COCO Detection Results with Mask-RCNN.

Model	Box AP	Mask AP	Latency (ms)
ResNet-50	39.0	34.8	818.9
ResNet-101	42.9	37.7	883.8
NFNet-F0	46.7	40.9	968.5
NFNet-F1	48.1	41.7	1411.4

optimize unnormalized networks with strong data augmentations. Leveraging this technique and simple architecture design principles, we develop a family of models which attain state-of-the-art performance on ImageNet without extra data, while being substantially faster to train than competing approaches. We also show that Normalizer-Free models are better suited to fine-tuning after pre-training on very large scale datasets than their batch-normalized counterparts.

## Acknowledgements

We would like to thank Aäron van den Oord, Sander Dieleman, Erich Elsen, Guillaume Desjardins, Michael Figurnov, Nikolay Savinov, Omar Rivasplata, Relja Arandjelović, and Rishub Jain for helpful discussions and guidance. Additionally, we would like to thank Blake Hechtman, Tim Shen, Peter Hawkins, and James Bradbury for assistance with developing highly performant JAX code.

## References

Arpit, D., Zhou, Y., Kota, B., and Govindaraju, V. Normalization propagation: A parametric technique for removing internal covariate shift in deep networks. In *International Conference on Machine Learning*, pp. 1168–1176, 2016.

Ba, J. L., Kiros, J. R., and Hinton, G. E. Layer normalization. *arXiv preprint arXiv:1607.06450*, 2016.

Babuschkin, I., Baumli, K., Bell, A., Bhupatiraju, S., Bruce, J., Buchlovsky, P., Budden, D., Cai, T., Clark, A., Danihelka, I., Fantacci, C., Godwin, J., Jones, C., Hennigan,

T., Hessel, M., Kapturowski, S., Keck, T., Kemaev, I., King, M., Martens, L., Mikulik, V., Norman, T., Quan, J., Papamakarios, G., Ring, R., Ruiz, F., Sanchez, A., Schneider, R., Sezener, E., Spencer, S., Srinivasan, S., Stokowiec, W., and Viola, F. The DeepMind JAX Ecosystem, 2020. URL <http://github.com/deepmind>.

Bachlechner, T., Majumder, B. P., Mao, H. H., Cottrell, G. W., and McAuley, J. Rezero is all you need: Fast convergence at large depth. *arXiv preprint arXiv:2003.04887*, 2020.

Balduzzi, D., Frean, M., Leary, L., Lewis, J., Ma, K. W.-D., and McWilliams, B. The shattered gradients problem: If resnets are the answer, then what is the question? In *International Conference on Machine Learning*, pp. 342–350, 2017.

Bello, I. Lambdanetworks: Modeling long-range interactions without attention. In *International Conference on Learning Representations ICLR*, 2021. URL <https://openreview.net/forum?id=xTJEN-gg1lb>.

Bernstein, J., Vahdat, A., Yue, Y., and Liu, M.-Y. On the distance between two neural networks and the stability of learning. *arXiv preprint arXiv:2002.03432*, 2020.

Bjorck, N., Gomes, C. P., Selman, B., and Weinberger, K. Q. Understanding batch normalization. In *Advances in Neural Information Processing Systems*, pp. 7694–7705, 2018.

Bradbury, J., Frostig, R., Hawkins, P., Johnson, M. J., Leary, C., Maclaurin, D., and Wanderman-Milne, S. JAX: composable transformations of Python+NumPy programs, 2018. URL <http://github.com/google/jax>.

Brock, A., De, S., and Smith, S. L. Characterizing signal propagation to close the performance gap in unnormalized resnets. In *9th International Conference on Learning Representations, ICLR*, 2021.

Chen, T., Kornblith, S., Norouzi, M., and Hinton, G. A simple framework for contrastive learning of visual representations. In *International conference on machine learning*, pp. 1597–1607. PMLR, 2020.

Cubuk, E. D., Zoph, B., Shlens, J., and Le, Q. V. Randaugment: Practical automated data augmentation with a reduced search space. In *Proceedings of the IEEE/CVF Conference on Computer Vision and Pattern Recognition Workshops*, pp. 702–703, 2020.

De, S. and Smith, S. Batch normalization biases residual blocks towards the identity function in deep networks. *Advances in Neural Information Processing Systems*, 33, 2020.

- Dosovitskiy, A., Beyer, L., Kolesnikov, A., Weissenborn, D., Zhai, X., Unterthiner, T., Dehghani, M., Minderer, M., Heigold, G., Gelly, S., Uszkoreit, J., and Houshy, N. An image is worth 16x16 words: Transformers for image recognition at scale. In *9th International Conference on Learning Representations, ICLR*, 2021. URL <https://openreview.net/forum?id=YicbFdNTTy>.
- Foret, P., Kleiner, A., Mobahi, H., and Neyshabur, B. Sharpness-aware minimization for efficiently improving generalization. In *9th International Conference on Learning Representations, ICLR*, 2021. URL <https://openreview.net/forum?id=6TmlmposlRM>.
- Ghiasi, G., Cui, Y., Srinivas, A., Qian, R., Lin, T.-Y., Cubuk, E. D., Le, Q. V., and Zoph, B. Simple copy-paste is a strong data augmentation method for instance segmentation. *arXiv preprint arXiv:2012.07177*, 2020.
- Gitman, I. and Ginsburg, B. Comparison of batch normalization and weight normalization algorithms for the large-scale image classification. *arXiv preprint arXiv:1709.08145*, 2017.
- Gong, C., Ren, T., Ye, M., and Liu, Q. Maxup: A simple way to improve generalization of neural network training. *arXiv preprint arXiv:2002.09024*, 2020.
- Google. Cloud TPU Performance Guide. <https://cloud.google.com/tpu/docs/performance-guide>, 2021.
- Goyal, P., Dollár, P., Girshick, R., Noordhuis, P., Wesolowski, L., Kyrola, A., Tulloch, A., Jia, Y., and He, K. Accurate, large minibatch sgd: Training imagenet in 1 hour. *arXiv preprint arXiv:1706.02677*, 2017.
- Gueguen, L., Sergeev, A., Kadlec, B., Liu, R., and Yosinski, J. Faster neural networks straight from jpeg. *Advances in Neural Information Processing Systems*, 31:3933–3944, 2018.
- Hanin, B. and Rolnick, D. How to start training: The effect of initialization and architecture. In *Advances in Neural Information Processing Systems*, pp. 571–581, 2018.
- Harris, C. R., Millman, K. J., van der Walt, S. J., Gommers, R., Virtanen, P., Cournapeau, D., Wieser, E., Taylor, J., Berg, S., Smith, N. J., Kern, R., Picus, M., Hoyer, S., van Kerkwijk, M. H., Brett, M., Haldane, A., del Río, J. F., Wiebe, M., Peterson, P., Gérard-Marchant, P., Sheppard, K., Reddy, T., Weckesser, W., Abbasi, H., Gohlke, C., and Oliphant, T. E. Array programming with numpy. *Nature*, 585(7825):357–362, Sep 2020. ISSN 1476-4687.
- He, K., Zhang, X., Ren, S., and Sun, J. Identity mappings in deep residual networks. In *European conference on computer vision*, pp. 630–645. Springer, 2016a.
- He, K., Zhang, X., Ren, S., and Sun, J. Deep residual learning for image recognition. In *CVPR*, 2016b.
- He, K., Gkioxari, G., Dollár, P., and Girshick, R. Mask r-cnn. In *Proceedings of the IEEE international conference on computer vision*, pp. 2961–2969, 2017.
- He, K., Fan, H., Wu, Y., Xie, S., and Girshick, R. Momentum contrast for unsupervised visual representation learning. In *Proceedings of the IEEE/CVF Conference on Computer Vision and Pattern Recognition*, pp. 9729–9738, 2020.
- He, T., Zhang, Z., Zhang, H., Zhang, Z., Xie, J., and Li, M. Bag of tricks for image classification with convolutional neural networks. In *Proceedings of the IEEE Conference on Computer Vision and Pattern Recognition*, pp. 558–567, 2019.
- Hendrycks, D. and Gimpel, K. Gaussian error linear units (GELUs). *arXiv preprint arXiv:1606.08415*, 2016.
- Hennigan, T., Cai, T., Norman, T., and Babuschkin, I. Haiku: Sonnet for JAX, 2020. URL <http://github.com/deepmind/dm-haiku>.
- Hoffer, E., Hubara, I., and Soudry, D. Train longer, generalize better: closing the generalization gap in large batch training of neural networks. In *Advances in Neural Information Processing Systems*, pp. 1731–1741, 2017.
- Hooker, S. The hardware lottery. *arXiv preprint arXiv:2009.06489*, 2020.
- Hu, J., Shen, L., and Sun, G. Squeeze-and-excitation networks. In *Proceedings of the IEEE conference on computer vision and pattern recognition*, pp. 7132–7141, 2018.
- Huang, G., Sun, Y., Liu, Z., Sedra, D., and Weinberger, K. Q. Deep networks with stochastic depth. In *European conference on computer vision*, pp. 646–661. Springer, 2016.
- Huang, L., Liu, X., Liu, Y., Lang, B., and Tao, D. Centered weight normalization in accelerating training of deep neural networks. In *Proceedings of the IEEE International Conference on Computer Vision*, pp. 2803–2811, 2017.
- Huang, L., Qin, J., Zhou, Y., Zhu, F., Liu, L., and Shao, L. Normalization techniques in training dnns: Methodology, analysis and application. *arXiv preprint arXiv:2009.12836*, 2020.
- Ioffe, S. Batch renormalization: Towards reducing minibatch dependence in batch-normalized models. *arXiv preprint arXiv:1702.03275*, 2017.

- Ioffe, S. and Szegedy, C. Batch normalization: Accelerating deep network training by reducing internal covariate shift. In *ICML*, 2015.
- Jacot, A., Gabriel, F., and Hongler, C. Freeze and chaos for dnns: an ntk view of batch normalization, checkerboard and boundary effects. *arXiv preprint arXiv:1907.05715*, 2019.
- Kaplan, J., McCandlish, S., Henighan, T., Brown, T. B., Chess, B., Child, R., Gray, S., Radford, A., Wu, J., and Amodei, D. Scaling laws for neural language models. *arXiv preprint arXiv:2001.08361*, 2020.
- Kolesnikov, A., Beyer, L., Zhai, X., Puigcerver, J., Yung, J., Gelly, S., and Houlsby, N. Large scale learning of general visual representations for transfer. *arXiv preprint arXiv:1912.11370*, 2019.
- Krizhevsky, A., Sutskever, I., and Hinton, G. E. Imagenet classification with deep convolutional neural networks. *Advances in neural information processing systems*, 25: 1097–1105, 2012.
- LeCun, Y. A., Bottou, L., Orr, G. B., and Müller, K.-R. Efficient backprop. In *Neural networks: Tricks of the trade*, pp. 9–48. Springer, 2012.
- Lin, T.-Y., Maire, M., Belongie, S., Hays, J., Perona, P., Ramanan, D., Dollár, P., and Zitnick, C. L. Microsoft coco: Common objects in context. In *European conference on computer vision*, pp. 740–755. Springer, 2014.
- Lin, T.-Y., Dollár, P., Girshick, R., He, K., Hariharan, B., and Belongie, S. Feature pyramid networks for object detection. In *Proceedings of the IEEE conference on computer vision and pattern recognition*, pp. 2117–2125, 2017.
- Loshchilov, I. and Hutter, F. Sgdr: Stochastic gradient descent with warm restarts. *arXiv preprint arXiv:1608.03983*, 2016.
- Loshchilov, I. and Hutter, F. Decoupled weight decay regularization. *arXiv preprint arXiv:1711.05101*, 2017.
- Luo, P., Wang, X., Shao, W., and Peng, Z. Towards understanding regularization in batch normalization. *arXiv preprint arXiv:1809.00846*, 2018.
- Mahajan, D., Girshick, R., Ramanathan, V., He, K., Paluri, M., Li, Y., Bharambe, A., and Van Der Maaten, L. Exploring the limits of weakly supervised pretraining. In *Proceedings of the European Conference on Computer Vision ECCV*, pp. 181–196, 2018.
- Merity, S., Keskar, N. S., and Socher, R. Regularizing and optimizing LSTM language models. In *International Conference on Learning Representations*, 2018.
- Nesterov, Y. A method for unconstrained convex minimization problem with the rate of convergence  $o(1/k^2)$ . *Doklady AN USSR*, pp. (269), 543–547, 1983.
- Pascanu, R., Mikolov, T., and Bengio, Y. On the difficulty of training recurrent neural networks. In *International conference on machine learning*, pp. 1310–1318, 2013.
- Pham, H., Xie, Q., Dai, Z., and Le, Q. V. Meta pseudo labels. *arXiv preprint arXiv:2003.10580*, 2020.
- Pham, H. V., Lutellier, T., Qi, W., and Tan, L. Cradle: cross-backend validation to detect and localize bugs in deep learning libraries. In *2019 IEEE/ACM 41st International Conference on Software Engineering (ICSE)*, pp. 1027–1038. IEEE, 2019.
- Polyak, B. Some methods of speeding up the convergence of iteration methods. *USSR Computational Mathematics and Mathematical Physics*, pp. 4(5):1–17, 1964.
- Qiao, S., Wang, H., Liu, C., Shen, W., and Yuille, A. Weight standardization. *arXiv preprint arXiv:1903.10520*, 2019.
- Qin, J., Fang, J., Zhang, Q., Liu, W., Wang, X., and Wang, X. Resizemix: Mixing data with preserved object information and true labels. *arXiv preprint arXiv:2012.11101*, 2020.
- Radford, A., Metz, L., and Chintala, S. Unsupervised representation learning with deep convolutional generative adversarial networks. In *4th International Conference on Learning Representations, ICLR*, 2016.
- Radosavovic, I., Kosaraju, R. P., Girshick, R., He, K., and Dollár, P. Designing network design spaces. In *Proceedings of the IEEE/CVF Conference on Computer Vision and Pattern Recognition*, pp. 10428–10436, 2020.
- Raghu, M., Gilmer, J., Yosinski, J., and Sohl-Dickstein, J. Svcca: Singular vector canonical correlation analysis for deep learning dynamics and interpretability. *Advances in neural information processing systems*, 30:6076–6085, 2017a.
- Raghu, M., Poole, B., Kleinberg, J., Ganguli, S., and Sohl-Dickstein, J. On the expressive power of deep neural networks. In *international conference on machine learning*, pp. 2847–2854. PMLR, 2017b.
- Robbins, H. and Monro, S. A stochastic approximation method. *The Annals of Mathematical Statistics*, pp. 22(3):400–407, 1951.
- Rota Bulò, S., Porzi, L., and Kotschieder, P. In-place activated batchnorm for memory-optimized training of dnns. In *Proceedings of the IEEE Conference on Computer Vision and Pattern Recognition*, pp. 5639–5647, 2018.

- Russakovsky, O., Deng, J., Su, H., Krause, J., Satheesh, S., Ma, S., Huang, Z., Karpathy, A., Khosla, A., Bernstein, M., Berg, A. C., and Fei-Fei, L. ImageNet large scale visual recognition challenge. *IJCV*, 115:211–252, 2015.
- Sandler, M., Howard, A., Zhu, M., Zhmoginov, A., and Chen, L.-C. Mobilenetv2: Inverted residuals and linear bottlenecks. In *Proceedings of the IEEE conference on computer vision and pattern recognition*, pp. 4510–4520, 2018.
- Sandler, M., Baccash, J., Zhmoginov, A., and Howard, A. Non-discriminative data or weak model? on the relative importance of data and model resolution. In *Proceedings of the IEEE/CVF International Conference on Computer Vision Workshops*, pp. 0–0, 2019.
- Santurkar, S., Tsipras, D., Ilyas, A., and Madry, A. How does batch normalization help optimization? In *Advances in Neural Information Processing Systems*, pp. 2483–2493, 2018.
- Shao, J., Hu, K., Wang, C., Xue, X., and Raj, B. Is normalization indispensable for training deep neural network? *Advances in Neural Information Processing Systems*, 33, 2020.
- Shen, S., Yao, Z., Gholami, A., Mahoney, M., and Keutzer, K. Powernorm: Rethinking batch normalization in transformers. In *International Conference on Machine Learning*, pp. 8741–8751. PMLR, 2020.
- Simonyan, K. and Zisserman, A. Very deep convolutional networks for large-scale image recognition. In *3rd International Conference on Learning Representations, ICLR*, 2015.
- Singh, S. and Shrivastava, A. Evalnorm: Estimating batch normalization statistics for evaluation. In *Proceedings of the IEEE/CVF International Conference on Computer Vision*, pp. 3633–3641, 2019.
- Smith, S., Elsen, E., and De, S. On the generalization benefit of noise in stochastic gradient descent. In *International Conference on Machine Learning*, pp. 9058–9067. PMLR, 2020.
- Srinivas, A., Lin, T.-Y., Parmar, N., Shlens, J., Abbeel, P., and Vaswani, A. Bottleneck transformers for visual recognition. *arXiv preprint arXiv:2101.11605*, 2021.
- Srivastava, N., Hinton, G., Krizhevsky, A., Sutskever, I., and Salakhutdinov, R. Dropout: a simple way to prevent neural networks from overfitting. *The Journal of Machine Learning Research*, 15(1):1929–1958, 2014.
- Srivastava, R. K., Greff, K., and Schmidhuber, J. Highway networks. *arXiv preprint arXiv:1505.00387*, 2015.
- Summers, C. and Dinneen, M. J. Four things everyone should know to improve batch normalization. *arXiv preprint arXiv:1906.03548*, 2019.
- Sun, C., Shrivastava, A., Singh, S., and Gupta, A. Revisiting unreasonable effectiveness of data in deep learning era. In *ICCV*, 2017.
- Sutskever, I., Martens, J., Dahl, G., and Hinton, G. On the importance of initialization and momentum in deep learning. In *International conference on machine learning*, pp. 1139–1147, 2013.
- Szegedy, C., Ioffe, S., Vanhoucke, V., and Alemi, A. Inception-v4, inception-resnet and the impact of residual connections on learning. *arXiv preprint arXiv:1602.07261*, 2016a.
- Szegedy, C., Vanhoucke, V., Ioffe, S., Shlens, J., and Wojna, Z. Rethinking the inception architecture for computer vision. In *2016 IEEE Conference on Computer Vision and Pattern Recognition (CVPR)*, pp. 2818–2826, 2016b.
- Tan, M. and Le, Q. Efficientnet: Rethinking model scaling for convolutional neural networks. In *International Conference on Machine Learning*, pp. 6105–6114, 2019.
- Tieleman, T. and Hinton, G. Rmsprop: Divide the gradient by a running average of its recent magnitude. *COURS-ERA: Neural networks for machine learning*, pp. 4(2):26–31, 2012.
- Touvron, H., Vedaldi, A., Douze, M., and Jégou, H. Fixing the train-test resolution discrepancy. In *Advances in Neural Information Processing Systems*, pp. 8252–8262, 2019.
- Touvron, H., Cord, M., Douze, M., Massa, F., Sablayrolles, A., and Jégou, H. Training data-efficient image transformers & distillation through attention. *arXiv preprint arXiv:2012.12877*, 2020.
- Vaswani, A., Shazeer, N., Parmar, N., Uszkoreit, J., Jones, L., Gomez, A. N., Kaiser, L., and Polosukhin, I. Attention is all you need. *arXiv preprint arXiv:1706.03762*, 2017.
- Wu, Y. and He, K. Group normalization. In *Proceedings of the European Conference on Computer Vision (ECCV)*, pp. 3–19, 2018.
- Xie, Q., Luong, M.-T., Hovy, E., and Le, Q. V. Self-training with noisy student improves imagenet classification. In *Proceedings of the IEEE/CVF Conference on Computer Vision and Pattern Recognition*, pp. 10687–10698, 2020.
- Xie, S., Girshick, R., Dollár, P., Tu, Z., and He, K. Aggregated residual transformations for deep neural networks. In *Proceedings of the IEEE conference on computer vision and pattern recognition*, pp. 1492–1500, 2017.

- Yang, G., Pennington, J., Rao, V., Sohl-Dickstein, J., and Schoenholz, S. S. A mean field theory of batch normalization. *arXiv preprint arXiv:1902.08129*, 2019.
- You, Y., Gitman, I., and Ginsburg, B. Large batch training of convolutional networks. *arXiv preprint arXiv:1708.03888*, 2017.
- You, Y., Li, J., Reddi, S., Hseu, J., Kumar, S., Bhojanapalli, S., Song, X., Demmel, J., Keutzer, K., and Hsieh, C.-J. Large batch optimization for deep learning: Training bert in 76 minutes. In *7th International Conference on Learning Representations, ICLR*, 2019.
- Yun, S., Han, D., Oh, S. J., Chun, S., Choe, J., and Yoo, Y. Cutmix: Regularization strategy to train strong classifiers with localizable features. In *Proceedings of the IEEE International Conference on Computer Vision*, pp. 6023–6032, 2019.
- Zhang, H., Cisse, M., Dauphin, Y. N., and Lopez-Paz, D. mixup: Beyond empirical risk minimization. *arXiv preprint arXiv:1710.09412*, 2017.
- Zhang, H., Dauphin, Y. N., and Ma, T. Fixup initialization: Residual learning without normalization. *arXiv preprint arXiv:1901.09321*, 2019a.
- Zhang, H., Goodfellow, I., Metaxas, D., and Odena, A. Self-attention generative adversarial networks. In *International conference on machine learning*, pp. 7354–7363. PMLR, 2019b.
- Zhang, J., He, T., Sra, S., and Jadbabaie, A. Why gradient clipping accelerates training: A theoretical justification for adaptivity. In *8th International Conference on Learning Representations, ICLR*, 2020. URL <https://openreview.net/forum?id=BJgnXpVYwS>.